Quantum chemical formulation of high-T_c superconductivity applied to α-FeSe

Itai Panas

Department of Chemistry and Biotechnology, Chalmers University of Technology, S-412 96 Gothenburg, Sweden
(Received 15 March 2010; revised manuscript received 11 July 2010; published 12 August 2010)

High-T_c superconductivity (HTS) in the cuprates is revisited and employed to interpret the superconductivity phenomenon in α-FeSe. HTS in α-FeSe is proposed to emerge from accidental near degeneracy among spin zero Fe^{2+} states on a magnetic sublattice in a magnetically inhomogeneous reference state illustrated by density-functional theory calculations. The spin zero Fe^{2+} ions sublattice is embedded in a second sublattice, which displays antiferromagnetic order. Existence of the latter enforces the former, and causes the violation of Hund´s rule. Detailed contact with the conceptual understanding of superconductivity in the cuprates is made.

I. INTRODUCTION

Superconductivity is arguably the most convincing and palpable macroscopic manifestation of quantum mechanics. Its potential use warrants interest every time a new class of superconductor is discovered. Today, the frontiers of technology include quantum computing based on macroscopic[1] as well as nanoscale qubits.[2] Often the concepts of superconductivity are employed to formulate the effective properties of entangled qubits. During some years, we have been investigating the complementary view point, that is, to formulate superconductivity in terms of entangled qubits.[3]

During the last 25 years, superconductivity has been discovered in the cuprate materials,[4] MgB_2 (Ref. [5]) and K_3C_{60}.[6] Besides these, a new family of materials has recently emerged, comprising the Fe pnictides,[7] here mainly referring to phosphides and arsenides. To date $Sm(O_{1-x}F_x)FeAs$ (Ref. [8]) is the pnictide which displays the highest critical temperature, 55 K. The simplest relative to the pnictide family is α-FeSe, which has $T_c \sim 8$ K at atmospheric pressure but acquires a T_c of 39 K at high pressures.[9] In the present study, superconductivity in α-FeSe will be discussed based on qualitative results from elementary density-functional theory (DFT) calculations in conjunction with a conceptual quantum chemical understanding of superconductivity developed for the cuprate superconductors.

In seeking to formulate the effective objects with complex inner structure, which produce superconductivity, we employ a strategy which views superconductivity as a "composite phenomenon" which emerges from the fusion of *a priori* symmetry broken elementary structures. Thus we take our inspiration from supercell calculations which allow for such symmetry breakings to take place, and we build our understanding of the effective behavior in terms of superpositions of such symmetry-broken elementary states. This allows us to focus on detailed properties of sublattices, which constitute the building blocks of the elementary symmetry-broken structures. We allow essences of the superconductivity to emerge from specific properties of these sublattices. This strategy was employed to understand the superconductivity in the cuprates,[10] and it is employed here to interpret the superconductivity observed in α-FeSe, the understanding of which may well have bearing on the mechanism for superconductivity in the Fe pnictides.

In the Fe pnictides as in α-FeSe, iron is considered to be the essential element for the superconductivity (see, e.g., Ref. [11], and references therein). This is apparently as opposed to the hole-doped cuprate superconductors where the charge carriers have been shown to reside on the oxygen ions.[12] Yet, it is the purpose of this work to formulate a possible common understanding of the two materials based on local signatures of accidental near degeneracy being required for achieving superconductivity. In case of the cuprates, the two different roles comprise accommodation of (a) the order parameter physics and (b) the charge carriers, provided by two different elements Cu and O. This is in contrast to the pnictides and selenide, where this multifunctionality is proposed to occur by magnetic symmetry breaking in the Fe^{2+} lattice producing (a) an antiferromagnetic (AFM) sublattice intertwined with (b) a nontrivial second sublattice made up of $S=0$ Fe^{2+} ions. Effective $S=0$ Fe^{2+} in a tetrahedral ligand field implies violation of Hund's rule as caused by the requirement of antiferromagnetic order in the second of the two sublattices. Such instabilities have been predicted for the Fe pnictides,[13,14] and in Ref. [13] the Hund's rule violation was emphasized, in particular.

This violation of Hund's rule implies that there may be other states which may accidentally have similar stabilities while displaying the same local spin and space symmetry. This "accidental degeneracy" enforced by the "confining" antiferromagnetic $S=\pm1$ sublattice is understood to allow for superconductivity to emerge as a result of nonadiabatic mixing of the locally incommensurate projected states by the phase coherent coupling to other equivalent local states elsewhere. It is from this collective phase that superconductivity emerges.

II. FORMAL CONSIDERATIONS

A. Computation

This study provides a qualitative possible understanding of key magnetic instabilities in α-FeSe of possible relevance also to the pnictides. It relies on the applicability of spin-polarized DFT within the Perdew-Burke-Ernzerhof generalized gradient approximation (GGA) (Ref. [15]) to represent the relevant magnetic states of the system addressed. This in turn implies that any ambiguity in choice of density func-

tional must be assumed not to influence the overall magnetic structure itself, and that qualitative evaluation of magnetic structures can be made in spite of the fact that ambiguity in relative stabilities of different magnetic structures still remains owing to the non-V representability of Kohn-Sham DFT for systems which display near degeneracy. The conclusions presented will be based on visual inspection of the 0.03 spin/Å^3 spin-density isosurfaces as computed by means of density functional theory. While simple and direct, yet it is noted that the spin density, similar to the electron density, is a reasonably robust property of DFT.

Here, we resort to Γ-point supercell calculations including 4 and 8 *a priori* symmetry-independent Fe ions. The reason for performing supercell calculations is in order to allow for magnetic symmetry breaking (*vide supra*). So-called semicore pseudopotentials[16] are employed to describe the core electrons while the valence electrons are described by a numerical double-zeta plus polarization function (DND) basis set. The calculations are performed by the DMOL3 software[17] in Material Studio, as provided by Accelrys Inc.

B. Overall relevance to superconductivity

Our understanding takes as starting point the fact that it is the collective phase in the London sense,[18] which causes superconductivity. The role of this collective phase is to ensure that a particular macroscopic ground state, produced by the coherent access of microscopic electronic states, is maintained. This particular macroscopic ground state allows the mixing of *a priori* incommensurate near-degenerate electronic states, and the stability of the resulting state is ensured by the coherence as manifested in the common phase among different microscopic systems. In order to make this point, in our discussion on the superconductivity in the cuprates, we formulated a real-space version[3,10] of the Bardeen-Cooper-Schrieffer theory.[19] Taking the independent particle reference state as point of departure, i.e. the electron gas, the quintessence of BCS theory is the electron correlation argument for the appearance of "pairs" [taken here to mean pair amplitudes] above the Fermi level. In our real space BCS formulation two *a priori* adiabatic narrow-gap subsystems automatically and independently display "pair amplitudes above the Fermi level." When coupled, the two subsystems each accesses *in addition* virtual pair-broken states. These latter nonadiabatic contributions to the correlated ground state are thus accessed by coupling the two small-gapped subsystems together. Thus, in our real space analog to the BCS theory the superconductivity is achieved by allowing for virtual pair-broken states to contribute to the correlated ground state, i.e., an extension of the BCS scenario is arrived at which accesses the superconductor state from the insulator side of a two-gap system.

Our formulation of superconductivity in the cuprates has one of the required gaps to be due to the charge carriers forming a checkerboard superstructure, which was later observed by scanning tunneling microscopy.[20] Given this checkerboard instability, which would be associated with the observed opening of a "pseudogap" at the Fermi level, i.e., local electronic near degeneracies displayed in each holes

cluster (cf. Ref. [21]), a second requirement also observed comprises the opening of a gap for spin fluctuations corresponding to short-range antiferromagnetic order.[22,23] The phase coherence of microscopic states producing superconductivity would be achieved by "phasing" holes cluster resonances in different plaqettes. The step by step evolution from an undoped cuprate material into a superconductor upon hole doping and subsequent decrease in temperature is depicted in Figs. [1(a)] and [1(b)]. Said phasing would be achieved by propagation of virtual magnetic excitations in a local antiferromagnetic background, i.e., virtual magnons, which would ensure the phase coherent access of local states on different plaquettes. In Ref. [10], we discussed the coupling of near-degenerate *a priori* incommensurate cluster states [see Figs. [1(c)] and [1(d)]] in terms of virtual pair-and-pair-broken local states. By allowing interplaquette phase coherent access of locally incommensurate states, a new macroscopic ground state was implied to form, where the electrodynamics of the resulting macroscopic phase would have superconductivity as consequence. Thus we produce this ground state not from the phases of some effective free electrons but from the phase coherent *access* of *a priori* incommensurate microscopic electronic *states*. The "microscopy" here refers to an effective few-electrons spectrum irrespective of in **r** or **k** space. In **k**-space linear momentum, single-electron eigenstates display apparent nonadiabaticity due to the Cooper pairing while in **r** space, the coupling of accidentally degenerate such incommensurate effective eigenstates of the angular momentum operator belonging to different irreducible representations are allowed to mix in each *a priori* gapped subsystem because virtual pair-breaking excitations become allowed to contribute to the ground state of each subsystem owing to the existence of the other complementary electronic subsystem.

In the cuprate superconductors, adopting a superatom language, the two locally incommensurate states display anisotropic S (nodeless) and $D_{x^2-y^2}$ symmetries, respectively, and thus the virtual pair-breaking excitation displays $D_{x^2-y^2}$ symmetry (cf. Refs. [10] and [24]). These two local states are allowed to contribute to the ground state owing to a particular spin fluctuation in the local antiferromagnetic background, i.e., a virtual magnon. The detailed phasing of virtual excitations in the charge carrier channel and the AFM background enforces a resulting order parameter. Hence, because of the rigidity of the short-range antiferromagnetic order, propagation of virtual spin fluctuation provides phase coherent coupling to a second local charge carrier state elsewhere. Thus an effective delocalization of a virtual pair-breaking excitation, i.e., the local mixing of virtual pair-and-pair-broken cluster states, is achieved. The delocalized pair resonance we interpret to be the Cooper pair.

C. Formal considerations

In order to understand this scenario in somewhat more formal terms, reference to the so-called periodic Anderson impurity model is helpful.[25] In what follows we assign the creation/annihilation operators σ^+/σ, and π^+/π for charge carriers in the AFM σ bands and local superatom π spaces, respectively. Consider the Hamiltonian,
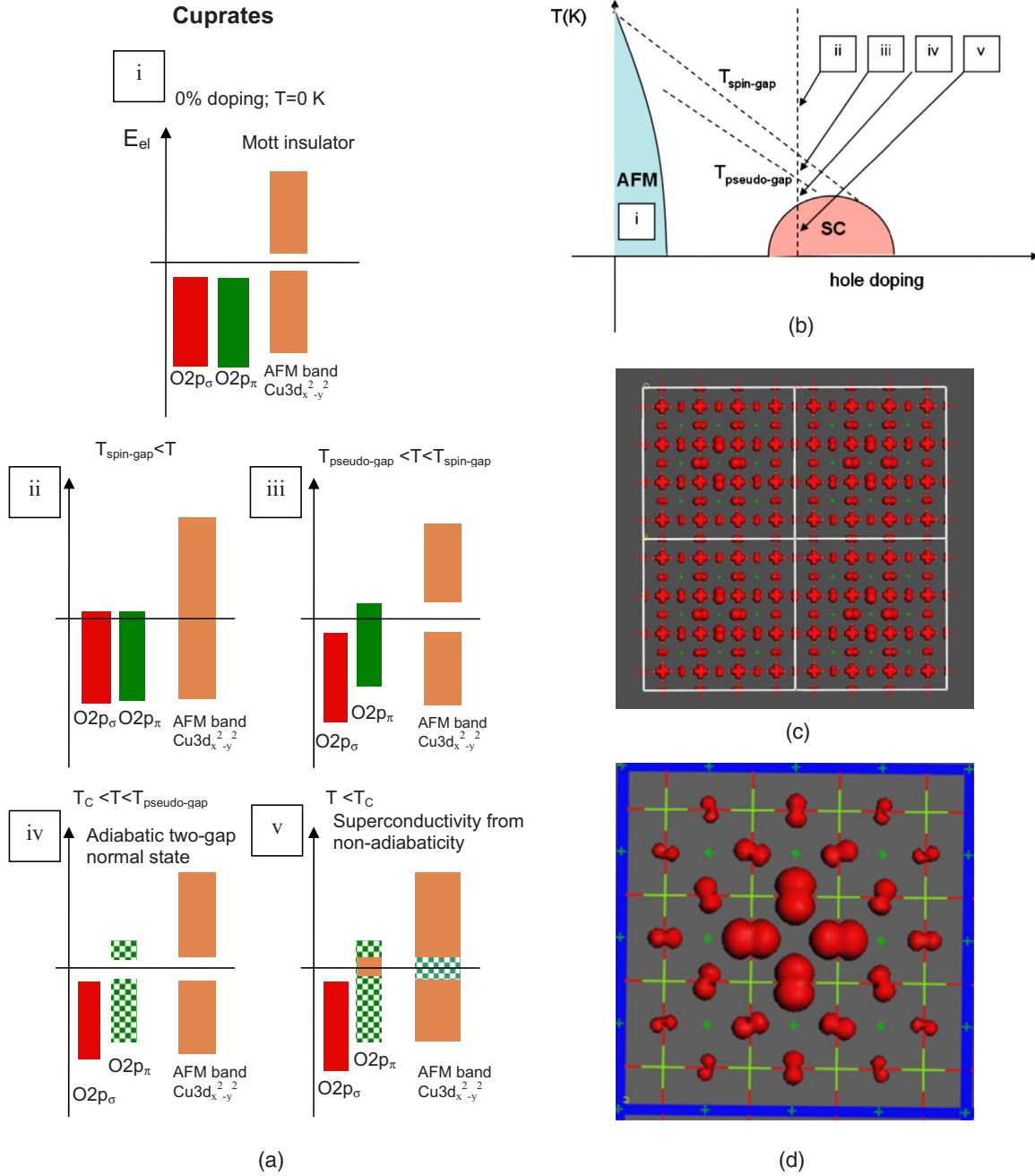
FIG. 1. (Color online) (a) Schematic representation of the proposed evolution from undoped antiferromagnetic insulator (i), into a hole-doped unconventional metal (ii), spin-gapped conductor (iii), pseudogapped and spin-gapped insulator (adiabatic two-gapped system) (iv), and finally into a superconductor (v) by allowing for nonadiabaticity in each subsystem by intersystem coupling as proposed in Ref. 10. Horizontal line represents the Fermi level. (b) The schematic phase diagram of the cuprates is shown where the different stages (i)–(v) are pointed out. (c) Checkerboard holes inhomogeneity in the spin density for which (Ref. 10) was formulated. Here in case of Hg-1201. Note population of O $2p$ π states. (d) One supercell as in (c) but replacing Cu^{2+} for Mg^{2+}.

$$\hat{H}_{red} = \hat{H}_{t\text{-}J}(\sigma) + \hat{H}_{transfer}(\sigma \leftrightarrow \pi : \vec{R}_{ion})$$
$$+ \hat{H}_{real\text{-}space\text{-}BCS}(\pi ; \vec{R}_{ion}) \tag{1a}$$

$$\hat{H}_{t\text{-}J}(\sigma) = \sum_{j,j',s} t_{jj'}(\sigma_{js}^+ \sigma_{j's} + \text{H.c.}) + J \sum_{\langle j,j' \rangle} \left(\vec{S}_j \cdot \vec{S}_{j'} - \tfrac{1}{4} n_j n_{j'} \right) \tag{1b}$$

such that the first two terms corresponds to the Anderson Model. The first term in Eq. (1a) is the t-J Hamiltonian,

which describes the doped AFM, which dominates at $T > T^*$. The "hybridization term,"

$$\hat{H}_{transfer}(\sigma \leftrightarrow \pi; \vec{R}_{ion}) = \sum_{i,j,L,s} V_{ijL}(\vec{R}_{ion}) \cdot (\pi^+_{iLs} \cdot \sigma_{js} + \sigma^+_{js} \cdot \pi_{iLs})$$

(1c)

allows for transfer of charge carriers from the σ band into cluster states of local π symmetry [see Figs. 1(c) and 1(d)], such that V_{ijL} includes the expansion coefficients for projection of said π states in terms of superatom states ("L" states, i.e., S, P, D, etc.). As previous stated, the detailed relative stabilities of σ and π states is determined by the local large cations (Ba, La, etc.) to plane distance. The transfer term [Eq. (1c)] becomes active at the spin-gap temperature [Fig. 1(a)iii]. Cooperative effects produce charge density wave signatures [Fig. 1(a)iv]. Finally, the real-space BCS term kicks in as it is responsible for the actual HTS at $T < T_c$. We write

$$\hat{H}_{real-BCS}(\pi; \vec{R}_{ion}) = \hat{H}_0(\pi; \vec{R}_{ion}) + \hat{H}_{coupling}(\pi; \vec{R}_{ion}),$$

(1d)

where

$$\hat{H}_0(\pi; \vec{R}_{ion}) = \sum_{i,L,s} \varepsilon_{iL}(\vec{R}_{ion}) \pi^+_{iLs} \pi_{iLs}$$

(1e)

and

$$\hat{H}_{coupling}(\pi; R_{ion}) = \frac{1}{2} \sum_{LL'ii'} (\pi^+_{iLs} \cdot \pi_{iL'(-s)} - \pi^+_{iL'(-s)} \cdot \pi_{iLs})$$
$$\cdot \langle M^{L_{i'}L'_i \Delta s_{i'}}_{L_i L'_i \Delta s_i}(R_{ion}; J) \rangle$$
$$\cdot (\pi^+_{i'L's} \cdot \pi_{i'L(-s)} - \pi^+_{i'L(-s)} \cdot \pi_{i'L's}).$$

(1f)

The purpose of the term (1f) is to mediate nonlocal cluster-cluster pair-making and pair-breaking resonances, i.e., inter-cluster entanglement while obeying local spin/symmetry constraints for the superatom and local AFM composite system. Thus, the wave-function ansatz, which matches Eqs. (1d)–(1f) mixes pair-and-pair-broken states. It does neither preserve spin nor space symmetry in the superatom subsystem spanned by the local π states. This is equivalently true for the magnetic σ subsystem. The two subsystems are said to be nonadiabatically coupled as represented by the coupling tensor **M** in Eq. (1f). More discussions on wave function properties are found in Refs. 10 and 26.

The crucial interplay between states of local σ and π symmetry makes our understanding *fundamentally* incompatible with any interpretation which takes HTS to be an exclusive single-band phenomenon. In particular, our understanding is incompatible with any mechanism of superconductivity in the cuprates, which assumes the Zhang-Rice singlet[27] to be essential for describing the superconductivity. While our understanding does state that the phenomenology of the single-band Hubbard model is useful in projecting out particular aspect of the HTS, it is emphasized that the full picture has nonadiabaticity between AFM and the checkerboard holes clusters (a) inducing magnon excitations in the
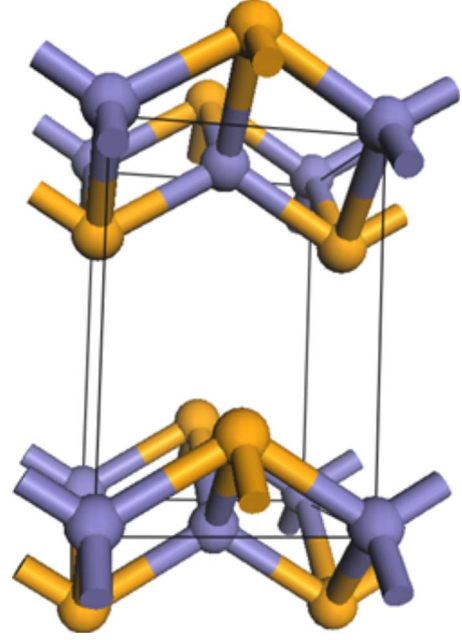

FIG. 2. (Color online) Chemical unit cell of α-FeSe.

AFM bands, and (b) causing pair-and-pair-broken charge carrier cluster states to mix.

A particular solution to Eq. (1d) was presented in Ref. 10 for the checkerboard superstructure in the hole-doped cuprates. That work preceded the discovery of the checkerboard structure by some 5 years. In this context, the present effort will attempt to formulate the corresponding understanding for α-FeSe (vide infra). Realization of a complementary resonating valence bond perspective in conjunction with Bose-Einstein condensation is discussed in detail in Ref. 26. In what follows, signatures of symmetry breaking in electronic subsystems as well as accidental local electronic near degeneracy on a sublattice is proposed to be valid for α-FeSe, and the above conceptual understanding of the superconductivity is applied in some detail.

α-FeSe *superconductivity—possible analog to the hole-doped cuprates*

α-FeSe was first synthesized by Hägg and Kindström.[28] The chemical unit cell of α-FeSe (Fig. 2) is, in principle, sufficient for antiferromagnetism to emerge. This is because the chemical unit cell allows for two symmetry-independent magnetic ions per plane. Let the antiferromagnetic property be the common property of the undoped cuprates and α-FeSe. An additional symmetry breaking is required in order to produce irons which represent the oxygen ions, on which the charge carriers reside in case of the cuprates. In order to allow for the equivalence of this, a superstructure which includes four magnetic centers is constructed. In Fig. 3, the spin density is plotted in case of eight symmetry independent Fe^{2+} ions as obtained in from a spin-polarized GGA calculation for a $2 \times 2 \times 1$ supercell of α-FeSe in the $S_{tot}=0$ state. It is remarkable to discover how the antiferromagnetic unit-cell size increases in order to accommodate a nontrivial $S=0$ (open shell singlet) Fe^{2+} ion sublattice. Implicitly it is
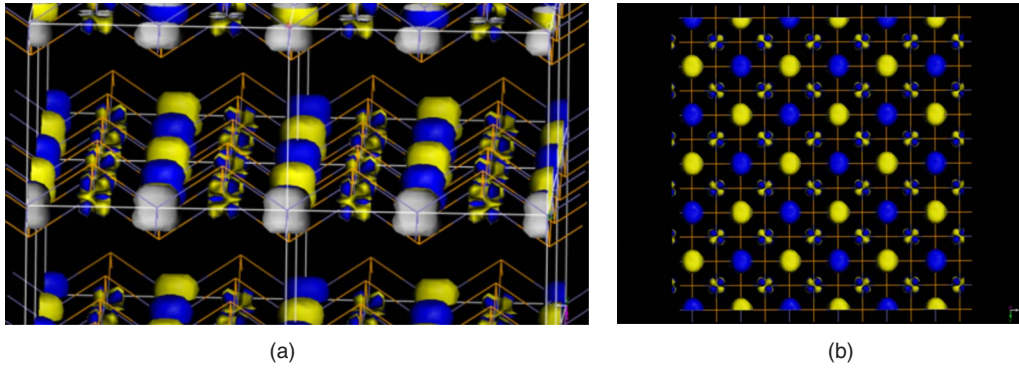
FIG. 3. (Color online) Spin density in magnetic 2×2 supercell. Global $S=0$ state, side view (a), top view (b). Four different Fe^{2+} ions are observed, two of antiphase $S=1$ and two magnetic antiphase $S=0$ local spin states.

understood that the "crossed" $S= \pm 1$ low-spin antiferromagnetic sublattices enforce the $S=0$ Fe^{2+} ions in the vertices. An interpretation of the electronic structures on each Fe^{2+} center, consistent with this understanding, is displayed in Figs. 4(a) and 4(b). It becomes interesting to compare this result with experiment. For $Fe_{1+d}Se_xTe_{1-x}$ Tranquada and co-workers[29] recently reported how, when static magnetism disappears and bulk superconductivity emerges, the spectral weight of the magnetic excitations shifts to the region of reciprocal space near the in-plane wave vector (0.5, 0.5) corresponding to the "collinear" "C-type" AFM configuration for the "two-Fe" unit cell (see Fig. 2). In Fig. 4(c), the relations between the C-type AFM structure (I), the "hidden" magnetic structure obtained here (II), as well as its "one-Fe-based unit cell" version (dashed in III) are represented schematically. It is gratifying to note that the "hidden
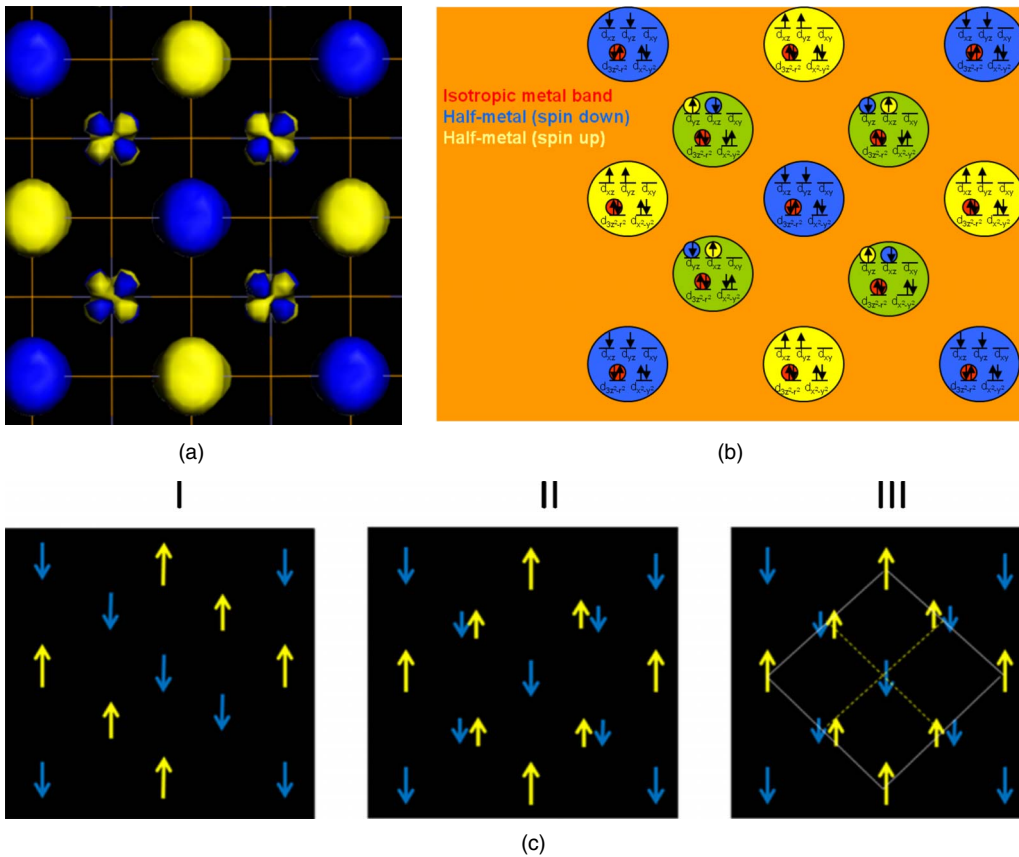

FIG. 4. (Color online) (a) Spin-density plot illustrating the composite magnetic structure. (b) Schematic population of the five d states (tetrahedral ligand field) on each Fe^{2+} ion in order to reproduce the magnetic 2×2 supercell (cf. Fig. 2). Note how the half-metallic property of alternating $S=-1$ (blue) and $S=1$ (yellow) in the diagonal directions are propagated through the $S=0$ (green) Fe^{2+} ions thus enforcing the violation of Hund's rule (small yellow and blue circles inside the green circles). Small red circles indicate what will become the charge carrier band upon self-doping [see Figs. 5(a) and 5(b) and text]. (c) The relation between the collinear C-type AFM structure (i), the magnetic structure obtained here (II), and the latter expressed in terms of the "one-Fe" unit cells (III) is displayed (see text).
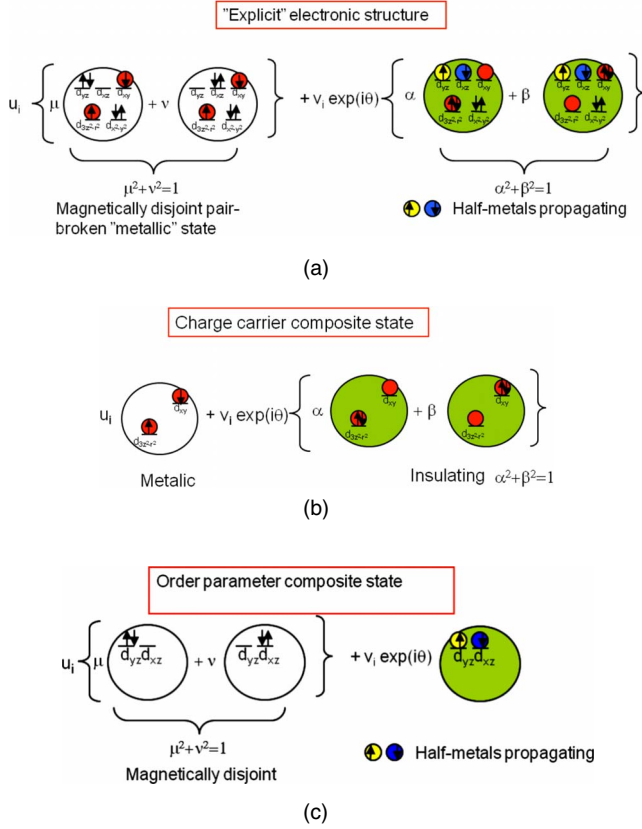
FIG. 5. (Color online) (a) The mixing of incommensurate electronic states is depicted in accord with our **r**-space understanding of BCS theory. The "explicit" representation shows the coupling of two pairs of incommensurate composite states associated with the violation of Hund's rule. The two depicted separately in (b) and (c). (b) The composite of incommensurate states which constitutes the charge carrier channel is depicted. Note the mix of the effective nodeless state (right term) with the state of $xy \times (3z^2 - r^2)$ symmetry (left). (c) The composite of incommensurate states which contains the order parameter is sketched. Note the effective mix of nodeless state (left term) with the state of $xy \times (3z^2 - r^2)$ symmetry (right) complementary to Fig. 5(b).

magnetic structure" investigated here is in agreement with said observed magnetic resonances in the vicinity of (0.5,0.5). Interestingly for the Fe pnictides said magnetic wave vector reflects the magnetic order in the parent compound as well as the positions of the magnetic resonances in the superconducting state.[30–32] Having said this, characteristic magnetic excitations should emerge at (0.5,0.5) in the one-Fe-based unit cell representation as well, obtained easiest by rotating the crystal by 45° and rescaling the lattice parameters, cf. Fig. 4(c:III) again. The fact that the $S=0$ Fe^{2+} ions display local singlet coupled open-shell electronic structures, i.e., violate Hund's rule, implies that these ions are destabilized by the surrounding antiferromagnetic structure (see Fig. 4 again). The destabilization of some Fe^{2+} ions to the extent that an open shell $S=0$ singlet state is accessed is suggested to imply that there are additional electronic configurations with $S=0$ which display similar energies, i.e., become accidentally near degenerate. This situation is analogous to the intraplaquette near-degenerate electronic

spectroscopy of the holes clusters in our formulation of cuprate superconductivity.

In what follows, a mechanism for superconductivity in α-FeSe is proposed, based on fluctuating magnetic superstructures of the form described in Fig. 3(b). We envisage two $S=0$ states, one which decouples the $S=0$ Fe^{2+} ion from the antiferromagnetic surrounding, and one which indeed does couple to the antiferromagnetic background [compare Figs. 4 and 5(a)]. In the sense of Eq. (1d), we apply the **r**-space formulation of BCS theory to produce a local superposition of two incommensurate pair-and-pair-broken states. Symmetry arguments suggest employing the $3d_{3z^2-r^2}$ and $3d_{xy}$ states and coupling to the local $3d_{xz}$ and $3d_{yz}$ states. Now we interpret the BCS wave function,

$$\prod_k \lfloor u_k + v_k e^{i\theta} c^+_{k\uparrow} c^+_{-k\downarrow} \rfloor |0\rangle \tag{2}$$

to mean

$$\prod_i \lfloor u_i(\mu \cdot c^+_{xz\uparrow} \cdot c^+_{xz\downarrow} + v \cdot c^+_{yz\uparrow} \cdot c^+_{yz\downarrow})|0\rangle_{OP} \cdot c^+_{zz\uparrow} \cdot c^+_{xy\downarrow}|0\rangle_{CC}$$

$$+ v_i e^{i\theta} \cdot c^+_{xz\uparrow} \cdot c^+_{yz\downarrow}|0\rangle_{OP} \cdot (\alpha \cdot c^+_{zz\uparrow} \cdot c^+_{zz\downarrow} + \beta \cdot c^+_{xy\uparrow} \cdot c^+_{xy\downarrow})$$

$$\times |0\rangle_{CC} \rfloor$$

$$u_i^2 + v_i^2 = 1, \quad \alpha^2 + \beta^2 = 1, \quad \text{and} \quad \mu^2 + v^2 = 1 \tag{3}$$

where $|0\rangle_{OP}$ and $|0\rangle_{CC}$ refer to the "order parameter" channel, providing the coupling to the AFM sublattice, and charge carrier degrees of freedom, respectively, and the index i points at the $S=0$ Fe^{2+} sites on the corresponding superlattice in real space [compare again Figs. 4 and 5(a)]. We make the obvious connection to Eq. (1) where the σ operators act on $|0\rangle_{OP}$, the π operators act on $|0\rangle_{CC}$, and the correlation term in Eq. (1) allows access to the real-space BCS ground state[10] or equivalently Bose-Einstein condensed Cooper pairs.[26] Note, in particular, how a correlated pair state in one orbital pair, coexists with a virtual pair-broken state in the other orbital pair on the same atom. From Eq. (3) the local manifestations of the charge carrier and order parameter degrees of freedom may be projected out, i.e.,

$$\prod_i [u_i \cdot c^+_{zz\uparrow} \cdot c^+_{xy\downarrow} + v_i e^{i\theta}(\alpha \cdot c^+_{zz\uparrow} \cdot c^+_{zz\downarrow} + \beta \cdot c^+_{xy\uparrow} \cdot c^+_{xy\downarrow})]|0\rangle_{CC}$$

$$u_i^2 + v_i^2 = 1, \quad \alpha^2 + \beta^2 = 1 \tag{4}$$

and

$$\prod_i [u_i(\mu \cdot c^+_{xz\uparrow} \cdot c^+_{xz\downarrow} + v \cdot c^+_{yz\uparrow} \cdot c^+_{yz\downarrow}) + v_i e^{i\theta} \cdot c^+_{xz\uparrow} \cdot c^+_{yz\downarrow}]|0\rangle_{OP}$$

$$\mu^2 + v^2 = 1, \quad u_i^2 + v_i^2 = 1 \tag{5}$$

corresponding to Figs. 5(b) and 5(c), respectively. In Eqs. (3)–(5), z^2, xy, xz, yz are short forms of $3d_{3z^2-r^2}, 3d_{xy}, 3d_{xz}$, and $3d_{yz}$, and the creation operators act at site i. We note that this separation and resulting signatures are equivalent to what was proposed for the cuprates in Ref. 10, meaning that where in Eq. (3) the symmetry of both terms is the same, this does not hold for either of the projected channels Eqs. (4)
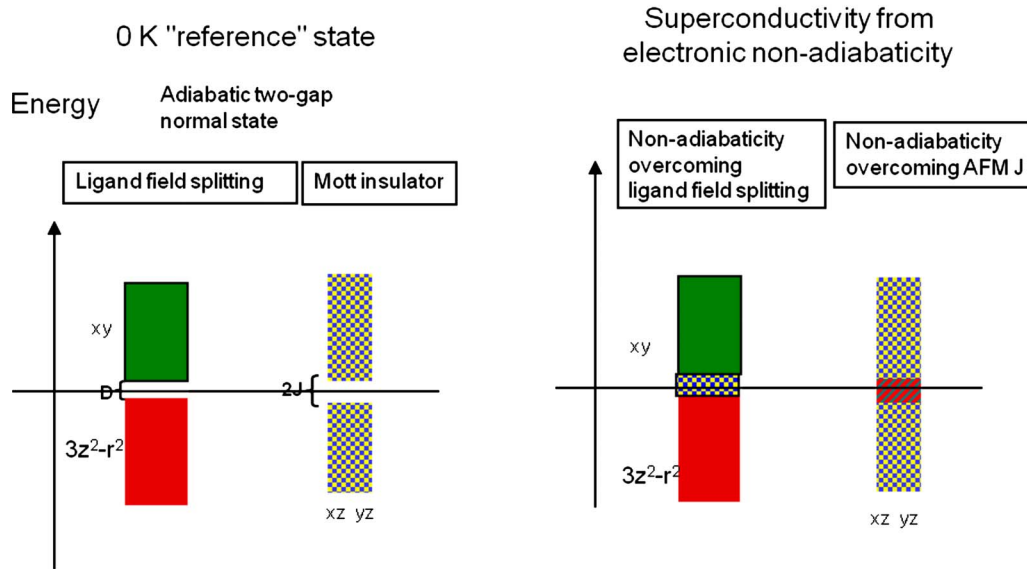
α-FeSe

FIG. 6. (Color online) Schematic representation of the transition from an adiabatic two-gap system to a superconductor, proposed to apply to a FeSe, is depicted [compare Figs. 1(a)iv and 1(a)v].

and (5), i.e., each mixing anisotropic S ($z^2 \cdot z^2$ and $xy \cdot xy$) with D ($z^2 \cdot xy$) symmetries. Because the $3d_{xz}$ and $3d_{yz}$ states connect to the antiferromagnetic background, these states are understood to mediate the phase information between equivalent sites (see Refs. 10 and 26). In particular, we observe the pair-breaking excitation to have effective $xy \times (3z^2 - r^2)$ symmetry [Fig. 5(b)]. Moreover, it is emphasized in Figs. 5(a)–5(c) how the accidental degeneracy among states allows the mixing of *a priori* incommensurate states in the $3d_{xz}$–$3d_{yz}$ and $3d_{3z^2-r^2}$–$3d_{xy}$ couples. We understand by inspection why it is required that the order-parameter symmetry [Fig. 5(c)] displays the symmetry of the virtual pair-breaking process [Fig. 5(b)]. Also to note is that the virtual pair-breaking excitation [Figs. 5(a) and 5(b)] comprises a mechanism for self-doping in the isotropic $3d_{3z^2-r^2}$ band, i.e., manifestation of superconductivity as a "virtual metal-insulator instability." The emergence of superconductivity in α-FeSe is depicted schematically in Fig. 6 (compare Fig. 1).

It is emphasized that neither the first nor the second term in Fig. 5(a) represents the "normal state." Rather, the two represent *a priori* different electron configurations which display the same spin and symmetry, and thus must mix by virtue of the variational principle of quantum mechanics. The resulting superfluid density becomes $v_i u_j u_i v_j$ where the indices refer to $S=0$ Fe^{2+} sites (see Ref. 26). It expresses how a pair state is shared by two sites, and states that a real-space Cooper pair amounts to a delocalized pair state among at least two such sites. Note, in particular, how the superfluid density vanishes if any of the four amplitudes is zero.

We make connection to the tentative understanding of the Fermi surfaces in the pnictides[33,34] by identifying the $3d_{3z^2-r^2}$ states to contribute the isotropic low-dispersive holelike metal band centered at the Γ point, and the $3d_{xz}$ and $3d_{yz}$ states to propagate the electron half-metal bands displaying

Fermi surfaces centered at the $(\pm \pi; \pm \pi)$ points, such that the resonances in Fig. 5 condition the mobilities of holelike and electronlike charge carriers. Thus, in our scenario all Fermi-surface segments couple in order to produce the superconductivity. This is because they are already coupled on each iron belonging to the $S=0$ Fe^{2+} sublattice (cf. Fig. 5 again).

Finally, while the superconducting order-parameter symmetry is unknown, it is presently believed to display $S_\pm$ symmetry (see, e.g., Refs. 35 and 36) as a means to connect the holelike and electronlike Fermi-surface segments (see, e.g., Ref. 34). What then does the $z^2 xy$ order-parameter symmetry obtained in the present study represent in this context? Connection is made to the $S_\pm$ symmetry by returning to Figs. 5(a) and 5(b), which display how virtual pair scattering occurs between $3d_{3z^2-r^2}$ and $3d_{xy}$ states (the small red circles in large green), and noting that this object (superposition of pair in $3d_{3z^2-r^2}$ and pair in $3d_{xy}$) displays the $S_\pm$ symmetry. Yet, it is the underlying $z^2 xy$ symmetry of the virtual pair-breaking excitations, common to the magnetic and charge carrier channels [compare Figs. 5(b) and 5(c)], which renders the superconducting pair-resonances coherence. It is gratifying to note that theoretical analysis based on all the five d bands in $LaFeAsO_{1-x}F_x$ by Kuroki *et al.*[37] suggests that a possible alternative to the $S_\pm$ order parameter symmetry[35,36] is D-wave pairing, i.e., $D_{x^2-y^2}$ in the reduced unit cell corresponding to D_{xy} in the original unit cell.

Interestingly, the superconductivity in α-FeSe is greatly enhanced upon applying pressure.[9] This is taken to indicate a strengthening of the superexchange interaction to further stabilize the antiferromagnetism in the confining sublattice. This in turn stabilizes the Hund's rule violated open shell states on the $S=0$ Fe^{2+} ions' sublattice. Were this understanding to be qualitatively true, then the reason for replacing Se^{2-} by As^{3-} is twofold. Invoking chemical pressure (a) enhances

the ligand-field splitting thus enforcing low-spin $S=\pm 1$ antiferromagnetism where formally $S=\pm 2$ would also be possible, and (b) stabilizes the AFM superstructure by enhancing the superexchange interaction which in turn further stabilizes the Hund's rule violating sublattice composed of $S=0$ Fe^{2+} ions. Finally we note that half of the Fe^{2+} ions have $|S|=1$ while the other half are $S=0$ ions. This formally implies an average spin $|\bar{S}|=\frac{1}{2}$ which may find qualitative support in the literature.[30]

III. CONCLUSION

Appearance of superconductivity in α-FeSe from a two-gapped semiconductor reference state is formulated in analogy to our understanding of superconductivity in the cuprates.[10] This analogy can be appreciated by comparing Figs. 1(a) and 6. A particular symmetry-broken magnetic structure has been described and proposed to provide the normal state from which superconductivity emerges in α-FeSe. It was understood to be composed of row-by-row antiphase half-metal bands along the $(\pm\pi;\pm\pi)$ directions. The low-spin $(S=\pm 1)$ antiferromagnetic sublattice was found to be intertwined with a sublattice composed of nontrivial magnetic $S=0$ Fe^{2+} ions. The exerted "magnetic pressure" on this sublattice causes the $S=0$ ions to violate Hund's rule. The existence of these open-shell $S=0$ ions in turn allows for the propagation of the antiphase magnetic structures along the $(\pm\pi;\pm\pi)$ directions. The existence of the magnetic $S=0$ sublattice is taken to imply that other $S=0$ Fe^{2+} states will have similar energies, so-called accidental degeneracy. It is this accidental degeneracy on the Fe^{2+} $S=0$ ions which drives the HTS owing to the "self-doping" away from perfect ferromagnetic occupations into the half-metal regime for each of the spin-up and spin-down rows [cf. Figs. 4(b), 4(c:III), and 5(a)].

This understanding finds essential features in common with our that of the cuprate superconductors, where consecutive symmetry lowering is observed as charge carrier and magnetic states separate first by occupying different bands, i.e., allowing for antiferromagnetism to develop by placing the charge carriers in disjoint oxygen bands, and subsequently allow for spatial electronic heterogeneity in order to produce accidentally degenerate states in both the magnetic and charge carrier channels. Mixes of incommensurate local states in each of the channels become locally allowed if the two channels couple. Because the antiferromagnetic band extends in space, it provides the means to phase coherently couple states at different sites. This understanding is identical to that produced here for α-FeSe.

More similarities between α-FeSe and the cuprate superconductors: (1) in both cases, the local mixing of accidental locally near-degenerate incommensurate electronic states produces the superconductivity. In case of the cuprates, the coupling of effective anisotropic S and $D_{x^2-y^2}$ states enforce an effective order parameter of $D_{x^2-y^2}$ symmetry in the antiferromagnetic band. In case of α-FeSe, a local $3d_{3z^2-r^2}$ state couples to $3d_{xy}$ thus requiring an $xy\times(3z^2-r^2)$ order-parameter symmetry.

(2) In both cases, scattering across the Fermi level in **k** space of conventional BCS theory, is replaced by the mixing of states qualitatively belonging to different eigenstates of the angular momentum operator.

(3) In both cases, the phase coherence is maintained by coupling to an antiferromagnetic background. In the cuprates, virtual excitations in the antiferromagnetic bands of $3d_{x^2-y^2}$ symmetry are matched to allow for the *a priori* nonadiabatic mixing of pair-and-pair-broken states in the charge carrier channel. In α-FeSe, these states are made up of $3d_{xz}$ and $3d_{yz}$ orbitals such that the symmetry of the product wave function becomes $xy\times z^2$ and the corresponding virtual pair-breaking excitation (closed-shell singlet→open-shell singlet) in the magnetic "order parameter channel," which propagates the phase, has $xy\times z^2$ symmetry corresponding to in-plane D_{xy} symmetry (Fig. 5, cf. Ref. 37). Having said this, it is noted how the correlated pair state depicted in Figs. 5(a) and 5(b) displays $S_\pm$ symmetry (red circles in larger green circles, cf. Ref. 35).

(4) In both cases, separability of atoms on which the charge carries reside from atoms which accommodate the antiferromagnetism emerges, i.e., $S=0$ Fe^{2+} ions in α-FeSe and the in-plane oxygen in case of the cuprates.

Finally, the key conceptual understanding of high critical temperature superconductivity from an insulator perspective is the incorporation of virtual pair-breaking excitations in the correlated many-body ground state. This manifestation of electronic nonadiabaticity reflects the coupling of two particular narrow-gapped electronic subsystems of which one has "superatomic" characteristics and the other displays short-range AFM correlations. This understanding of HTS shares central concepts with quantum random networks.[38] In the latter, entanglement of "superatom" qubits was to be accomplished by means of an external source of squeezed photons. Here the squeezed photons are replaced by innate virtual magnons in the local AFM "bath" surrounding the superatoms.

[1] J. Clarke and F. K. Wilhelm, Nature (London) **453**, 1031 (2008).

[2] H. J. Briegel, D. E. Browne, W. Dür, R. Raussendorf, and M. Van den Nest, Nat. Phys. **5**, 19 (2009).

[3] I. Panas, American Physics Society Proceedings, Miami, 1999, Vol. 483, p. 85.

[4] J. G. Bednorz and K. A. Müller, Z. Phys. B: Condens. Matter **64**, 189 (1986).

[5] J. Nagamatsu, N. Nakagawa, T. Muranaka, Y. Zenitani, and J.

Akimitsu, Nature (London) **410**, 63 (2001).

[6] A. F. Hebard, M. J. Rosseinsky, R. C. Haddon, D. W. Murphy, S. H. Glarum, T. T. M. Palstra, A. P. Ramirez, and A. R. Kortan, Nature (London) **350**, 600 (1991).

[7] Z. Wei, H. Li, W. L. Hong, Z. Lv, H. Wu, X. Guo, and K. Ruan, J. Supercond. Novel Magn. **21**, 213 (2008).

[8] Z.-A. Ren, W. Lu, J. Yang, W. Yi, X.-L. Shen, Z.-C. Li, G.-C. Che, X.-L. Dong, L.-L. Sun, F. Zhou, and Z.-X. Zhao, Chin. Phys. Lett. **25**, 2385 (2008).

[9] S. Margadonna, Y. Takabayashi, Y. Ohishi, Y. Mizuguchi, Y. Takano, T. Kagayama, T. Nakagawa, M. Takata, and K. Prassides, Phys. Rev. B **80**, 064506 (2009).

[10] I. Panas, J. Phys. Chem. B **103**, 10767 (1999).

[11] K. Ishida, Y. Nakai, and H. Hosono, J. Phys. Soc. Jpn. **78**, 062001 (2009).

[12] P. Abbamonte, L. Venema, A. Rusydi, G. A. Sawatzky, G. Logvenov, and I. Bozovic, Science **297**, 581 (2002).

[13] J. P. Rodriguez and E. H. Rezayi, Phys. Rev. Lett. **103**, 097204 (2009).

[14] F. Cricchio, O. Grånäs, and L. Nordström arXiv:0911.1342 (unpublished).

[15] J. P. Perdew, K. Burke, and M. Ernzerhof, Phys. Rev. Lett. **77**, 3865 (1996).

[16] B. Delley, Phys. Rev. B **66**, 155125 (2002).

[17] B. Delley, J. Chem. Phys. **92**, 508 (1990); **100**, 6107 (1996); **113**, 7756 (2000).

[18] F. London, Phys. Rev. **74**, 562 (1948).

[19] J. Bardeen, L. N. Cooper, and J. R. Schrieffer, Phys. Rev. **106**, 162 (1957).

[20] K. McElroy, D.-H. Lee, J. E. Hoffman, K. M. Lang, J. Lee, E. W. Hudson, H. Eisaki, S. Uchida, and J. C. Davis, Phys. Rev. Lett. **94**, 197005 (2005).

[21] G. Levy, M. Kugler, A. A. Manuel, Ø. Fischer, and M. Li, Phys. Rev. Lett. **95**, 257005 (2005).

[22] H. A. Mook, P. Dai, S. M. Hayden, G. Aeppli, T. G. Perring, and F. Dogan Nature (London) **395**, 580 (1998).

[23] R. Ofer, G. Bazalitsky, A. Kanigel, A. Keren, A. Auerbach, J. S. Lord, and A. Amato, Phys. Rev. B **74**, 220508(R) (2006).

[24] C. C. Tsuei, J. R. Kirtley, C. C. Chi, Lock-See Yu-Jahnes, A. Gupta, T. Shaw, J. Z. Sun, and M. B. Ketchen, Phys. Rev. Lett. **73**, 593 (1994).

[25] P. W. Anderson, Phys. Rev. **124**, 41 (1961).

[26] I. Panas (submitted).

[27] F. C. Zhang and T. M. Rice, Phys. Rev. B **37**, 3759 (1988).

[28] G. Hägg and A. L. Kindström, Z. Phys. Chem. **22**, 455 (1933).

[29] Z. Xu, J. Wen, G. Xu, Q. Jie, Z. Lin, Q. Li, S. Chi, D. Singh, G. Gu, and J. Tranquada, arXiv:1005.4856 (unpublished).

[30] C. de la Cruz, Q. Huang, J. W. Lynn, J. Li, W. Ratcliff II, J. L. Zarestky, H. A. Mook, G. F. Chen, J. L. Luo, N. L. Wang, and P. Dai, Nature (London) **453**, 899 (2008).

[31] W. Yin, C. Lee, and W. Ku, arXiv:1003.0512 (unpublished).

[32] S. Li et al., Phys. Rev. B **79**, 054503 (2009).

[33] A. Subedi, L. Zhang, D. J. Singh, and M.-H. Du, Phys. Rev. B **78**, 134514 (2008).

[34] D. J. Singh, Physica C **469**, 418 (2009).

[35] I. I. Mazin, D. J. Singh, M. D. Johannes, and M. H. Du, Phys. Rev. Lett. **101**, 057003 (2008).

[36] I. I. Mazin, Nature (London) **464**, 183 (2010).

[37] K. Kuroki, S. Onari, R. Arita, H. Usui, Y. Tanaka, H. Kontani, and H. Aoki, Phys. Rev. Lett. **101**, 087004 (2008).

[38] S. Perseguers, M. Lewenstein, A. Acín, and J. I. Cirac, Nat. Phys. **6**, 539 (2010).